AIAA JOURNAL
Vol. 37, No. 6, June 1999

Soot Measurements in a Simulated Engine Exhaust Using Laser-Induced Incandescence

Richard T. Wainner* and Jerry M. Seitzman†
Georgia Institute of Technology, Atlanta, Georgia 30332-0150
and
Stefan R. Martin‡
MetroLaser, Inc., Irvine, California 92614-6428

Soot mass concentrations were measured with laser-induced incandescence (LII) in a nonreacting flow. The behavior of the LII signal with respect to soot concentration, particle size, and temperature was isolated with the use of a controllable soot-generating device. This device can simulate a hot, low-soot-concentration environment similar to that of a jet engine exhaust. Reduction of interference signals and high detection sensitivity were achieved with the use of a Nd:YAG laser at its fundamental wavelength and broadband detection from 570 to ~850 nm. The LII signals were nearly proportional to soot concentration over 4 orders of magnitude, with a soot detection limit of better than ~1 part per trillion (~2 $\mu g/m^3$). The detection setup was designed, according to a model of the LII process, to reduce dependence on local gas temperature and soot particle size. Experimental results agreed with the model predictions in terms of particle size dependence, and negligible temperature dependence (beyond gas density effects) was seen for gas temperatures from 70 to 300°C.

Introduction

SOOT produced in hydrocarbon combustion is a critical concern for engine designers and operators, both in the combustor and in the engine exhaust. Soot exhausts from diesel and jet engines are of particular interest because they are seen as an important source of soot emissions into the environment, especially when they are operating at off-design conditions. Because soot is a significant pollutant, for both human health and environmental reasons there is growing pressure for reductions in soot emissions. Also, soot measurements are useful for analysis and possibly active control of incomplete combustion.[1–3]

Whether for combustor monitoring or environmental impact, the exhaust of an engine represents the most convenient location to measure soot. Researchers have, in fact, been making measurements of exhaust components, including particulate matter, for a long time in a number of different ways. Most measurements of combustion-generated soot have been based on intrusive sampling or optical techniques, such as elastic scattering and extinction.[4–8] These methods, however, can suffer in the low-soot conditions typical of an engine exhaust. Sampling probes and gas samplers are intrusive, can require long sampling times, and have limited spatial resolution. Elastic scattering is sensitive to background scattering, e.g., from surfaces, and has a strong dependence on particle size, including agglomerate size. Extinction is a path-integrated technique, and requires approaches such as tomographic inversion to recover soot profile information. Also, extinction is insensitive at low soot concentrations because low extinction implies measurement of a small change in a large signal. For example, a laser beam through a meter pathlength of exhaust with 1 mg/m^3 soot exhibits only 1% extinction at 633 nm. In jet engine exhausts, the soot concentration, and thus the extinction, can be much lower, and beam steering can make extinction measurements difficult. Other methods for soot measurement include photoacoustic spectroscopy,[9] radiometry,[3] and photoelectron emission.[2]

Laser-induced incandescence (LII) has emerged as an attractive and versatile technique for the measurement of soot concentrations in unsteady flows of complex geometry. LII has been shown to be a robust technique that can produce instantaneous point, line, or planar measurements. Experimental studies have utilized LII for soot volume fraction measurement in gas and droplet flames[10–22] and in diesel engine cylinders[23] and exhaust.[24] Other experiments have generated carbon particles by means other than combustion,[25–27] and some examples exist where LII was employed for particle sizing.[21,26,27] Volume fraction calibrations of the LII signal have employed extinction measurements[11–18] or sampling methods.[10]

The versatility and the inherent challenges of LII are evidenced in the various means of generating and detecting the LII signal. Various approaches have attempted to minimize the interference from scattering (including Mie and Raman), the atomic or molecular emissions (PAH, C_2) typical of high-intensity visible excitation, and flame luminance (more noticeable at longer wavelengths). Some researchers have suggested that the long lifetime of the LII signal (compared to the interferences) may be exploited to avoid interfering signals by means of delayed detection.[15,22] However, models developed to understand the LII process have suggested that the incandescence at later times is more susceptible to variations in particle size and local gas temperature.[28–32] Alternatively, the model used in this research has shown that a short detection gate just after the laser pulse may be a good compromise.[32] Whereas soot volume fractions have been shown to be nearly proportional to promptly detected LII signals in a number of flames,[10,12–18] some discrepancies with extinction data have been noted.[13–15] Model results have indicated that this may result from a signal dependence on primary particle size.

Most of these previous LII measurements have been performed in flame environments with relatively high soot concentrations (ppm levels). A combusting environment is, however, complex and difficult to control. Even in a steady flame, spatial variations in temperature and chemistry are significant. Also, soot concentrations can be high enough to cause significant problems due to signal trapping. Thus, flames are a challenging environment for the quantitative understanding and calibration of the LII signal, and more significantly, flame conditions are not representative of the environment of an engine exhaust. LII has also been applied in diesel engine exhausts,[24] and reasonable results were obtained for the soot concentration range observed in that environment. However, uncertainties in the operating conditions and soot loading in this environment limit the ability to test the accuracy of standard LII models.

Presented as Paper 98-0398 at the AIAA 36th Aerospace Sciences Meeting, Reno, NV, Jan. 12–15, 1998; received April 14, 1998; revision received Nov. 18, 1998; accepted for publication Nov. 24, 1998.

*Graduate Research Assistant, School of Aerospace Engineering. Student Member AIAA.
†Assistant Professor, School of Aerospace Engineering. Member AIAA.
‡Senior Scientist, Particle Analysis, 18010 Skypark Circle, Suite 100.

In this paper, we compare LII measurements over a large range of soot concentrations and primary particle sizes in a controlled, high-temperature, but noncombusting environment. There are two primary goals. The first is the determination of the detection limits for LII in conditions similar to those of engine exhausts. The second involves testing the accuracy of current LII models, which are based on spherical soot particles. The facility that we employ allows accurate measurements over a wide range of carbon concentrations, with control over particle size. Because particle size will vary in exhausts, it is important to be able to predict size effects both for error estimation and for possible correction schemes.

LII Background

In general, when a soot particle absorbs energy from a laser beam, its temperature increases. With a sufficiently high energy absorption rate, the temperature will rise to levels where significant incandescence, essentially blackbody emission, and vaporization can occur. (For example, 3915 K is the approximate vaporization temperature for graphite.) One interesting aspect of the LII process is its dependence on laser energy above some threshold.[12,13,16,20,30] This threshold occurs when the laser intensity is sufficient to heat a soot particle to a point where vaporization dominates. Any further increase in laser intensity raises the average particle's temperature only slightly and primarily acts to vaporize more of the particle's mass. These are counteracting effects. The temperature rise increases the incandescence, but the mass loss reduces the signal. Together they cause the incandescence to be a weak function of laser energy above the threshold. A significant fraction of the increased average particle temperature may come from the wings of the laser spatial profile. More uniform profiles have shown a noted decrease in signal beyond the vaporization threshold.[12,16] The signal plateau for Gaussian beams is advantageous, reducing the importance of laser energy fluctuations or extinction across a flow.

Soot particles are, in general, branchy agglomerates of nominally spherical primary particles.[4] The LII signal is nearly proportional to volume fraction because the primary soot particles (and often even the agglomerates) are in the Rayleigh limit, i.e., they are much smaller than the laser excitation wavelength. The particles respond to the laser approximately as volume absorbers and emitters. However, the energy loss mechanisms of conduction and vaporization are expected to scale more like surface area d^2. Thus, it is predicted that primary particle size and gas temperature would affect the volumetric nature of the LII signal through these cooling mechanisms.

As mentioned, one of the goals of the experiment was to test the accuracy of standard LII models, especially with respect to the particle size dependence of the LII signal. These models entail an energy and mass balance that includes absorption of energy from the laser and the energy loss mechanisms of radiation, vaporization, and conduction. Generally, the temperature and particle size histories are calculated for an individual, homogeneous, spherical primary soot particle with no relative motion compared to the surrounding atmosphere and constant physical properties.[32]

The analysis by Melton[28] shows that, in the limit of negligible conduction and radiative losses, for a nearly constant particle temperature (near the vaporization temperature) and for low mass loss, the LII signal would scale as d^n with $n = 3 + 0.154/\lambda_{\text{detection}}$. This expression has usually been interpreted as indicating that longer detection wavelengths are preferable for accurate volume fraction ($\propto d^3$) measurements. This would also imply that the LII signal would underpredict f_v for small particles if calibrated in a flame or region with large soot particles. Experimental evidence of this particle size effect is unclear. The simple appearance of the small flames used in many LII experiments belies the complexities mentioned earlier of measurements in a combusting environment. Also, to date, the only method available for correcting for the signal trapping induced by the dense soot zones is tomographic inversion, which requires many measurements and a steady flowfield. Reliable data on size dependence in a controlled soot environment do not appear to exist.

Experimental Methods

Soot Generator

The combination of a controlled soot field and simulation of an engine exhaust was attained with the use of a soot generator[25] that provided an aerosol of carbon black particles (Fig. 1). The dryer tube is wrapped with heater tape to maintain approximately 100°C walls. The flow at the output of the generator is nonreacting, has no potential interferences associated with the presence of polycyclic aromatic hydrocarbons, and is dilute enough to avoid signal trapping. It is also designed to be nearly uniform in temperature, concentration, and particle size.

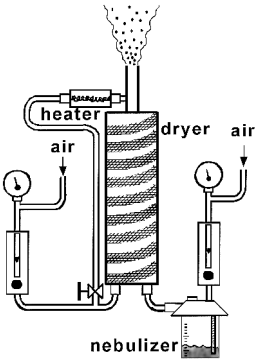

Fig. 1 Soot-generating experimental apparatus.

The aerosol was obtained in the following manner: A dispersion of carbon black (soot) in distilled water (5.6 g of C per liter of H_2O) was prepared with 1 ml of gum arabic (Winsor and Newton) added per liter of water as an emulsifier. This solution was atomized with the use of an aspirator/impingement-type nebulizer (Inspiron), providing a carbon/water fog. The solution was aspirated with air at a constant flow rate of 9.2 l/min, which yielded a solution flow rate of 0.34 ml/min. The nebulizer output was diluted by a secondary airflow rate, which varied between four flow rates: 315, 460, 770, and 1110 cm^3/s (based on standard temperature and pressure). Separate airflow rates were measured with calibrated rotameters and pressure gauge. The carbon black material (Cabot 800) is composed of approximately 17-nm particles with low aggregate structure, i.e., an aggregate diameter ~3 times the primary particle diameter (private communication, C. Beckman, Cabot Corporation, Boston, Massachusetts, Oct. 1998). Although less aggregated, this material should be similar in morphology and internal structure to aged (hydrocarbons desorbed) soot from engines.[33]

Each flow was separately directed into an aluminum drying cylinder (7.7-cm diameter, 61 cm long) held vertically. To evaporate the water droplets, the cylinder was heated with heating tape to a nominal temperature of 100°C. The resulting suspension of dry carbon particles exited the top of the drying cylinder out a 30-cm-long aluminum tube. This particle-laden jet was 15 mm in diameter, and measurements were made about 15 mm from the end of the tube. The exit temperature of the jet was also varied by preheating the secondary airflow by diverting some fraction of it through a coiled-filament heater (Sylvania; Process Heat). Exit temperatures ranged from 70 to 300°C, as measured by a type-K thermocouple.

Small variations (~3 times) in the carbon aerosol concentration were obtained by changing the secondary airflow rate. Greater reductions in carbon concentration were achieved by further diluting the carbon/water dispersion. This should, however, also change the size of the carbon particles produced. As the carbon-laden water droplet evaporates, surface tension and electrostatic forces cause all of the small carbon black particles to form a single, compact, nearly spherical particle (as evidenced by transmission electron microscopy data in Ref. 25) by the time the water is evaporated. Thus, the particle size at the exit of the generator should vary with the cube root of the concentration of the carbon solution. The nominal soot size is determined by assuming that each droplet produces a single soot particle. Thus, the particle sizes are simply a function of the liquid concentration and the size of the initial water droplets produced by the nebulizer. The water droplet size was constant for all conditions because the nebulizer flow was not varied, and the droplet sizes were measured by phase Doppler particle analysis (PDPA). Because of the similarity in carbon content between the particles produced by this device and aged soot from engine exhausts, we refer to the carbon aerosol as *soot*.

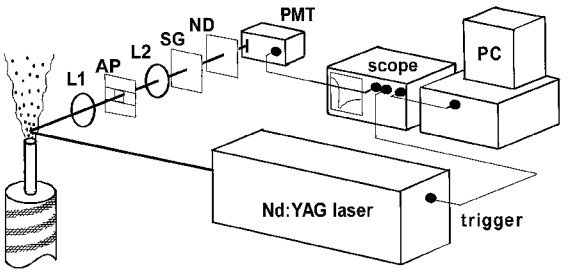

Fig. 2 LII experimental setup.

Optical System

The LII signal is produced by the fundamental output of a Nd:YAG laser [1064 nm, 7 ns full width at half-maximum (FWHM)] operated at 10 Hz. The data employed an unfocused, nominally Gaussian beam at 250 mJ. The beam diameter of 8 mm, measured by a burn mark method and Rayleigh scattering, provides an effective average illuminating energy density in the observed region between 0.5 and 1.0 J/cm^2, based on the FWHM of the beam. This laser fluence was beyond the threshold value required to make the LII signal nearly independent of laser fluence (discussed subsequently). The repeatability of pulse-to-pulse laser energy and temporal profile was generally good, with a worst case variation of $\pm 7\%$.

The LII signal was recorded at a right angle to the laser beam by a photomultiplier tube (PMT) (Hamamatsu R928B) behind the collection optics of 150- and 50-mm-focal-length spherical lenses for L1 and L2, respectively, and a height/width adjustable (AP) rectangular aperture (Fig. 2). The collection volume was approximately 8 mm wide × 3 mm high (defined by the aperture and centered vertically on the laser beam) and 8 mm deep (defined by the width of the laser beam). Optical filtering was applied to the imaged light just prior to the detector. Neutral density filters (ND; Fig. 2) were used to keep the PMT within its linear operating range. The spectral limits of the detection system were ~570 nm [set by OG550 and OG570 Schott glass filters (SG; Fig. 2)] to ~850 nm (the 1.0% quantum efficiency point of the PMT). This broad detection bandwidth, combined with a collection volume of ~0.2 cm^3, produced strong LII signals and, therefore, sensitive soot measurements. In addition, detection at longer wavelengths is predicted to reduce the particle size dependence of the signal, as described earlier.

The output current from the PMT was input to a digital oscilloscope (1-GHz sampling rate) that recorded the time-resolved LII signal up to 350 ns after the onset of the laser pulse and then stored it on a computer. All of the data are based on signals averaged over 128 laser pulses (~13-s averages with our 10-Hz laser). In addition, the reported LII signals were integrated over a 50-ns gate, beginning with the onset of the laser pulse, to isolate the LII occurring during the high-temperature, vaporization-dominated period of the incandescence. Modeling results indicate that this is an efficient way to minimize the particle size and gas temperature dependence of the LII.[32]

Results

The infrared output of the Nd:YAG laser was chosen over the frequently used green (532 nm) output to improve LII measurement of low-level soot concentrations. Previous experiments, performed in a diffusion flame, showed that infrared (IR) excitation is less likely to produce interference associated with laser-produced C_2 emission. More significantly, IR excitation can allow excellent rejection of elastic scattering, from the soot particles themselves or from surfaces, by employing visible signal detection and IR-blind detectors. Also, the longer excitation wavelength means that even larger agglomerate particles are more likely to be within the Rayleigh range for absorption.[28–32]

For LII measurements over a range of particle sizes, one must be certain that all of the particles are being heated to their vaporization temperature. Below the vaporization limit, there is a greater range to the temperatures reached by different sized particles. This problem is shown in Fig. 3, where model results are shown for the dynamic range of the signal per unit volume (or mass) of soot against energy fluence for a given particle size range. If particle size was not important, then the dynamic range of the signal normalized this way would be unity. This curve is another example of the threshold characteristic of the LII signal with increasing laser intensity. The dynamic range is calculated for particle diameters from 4 to 100 nm. (Although primary particle diameters rarely exceed 40 nm, agglomeration may increase the effective optical diameter.) The model results show that energy fluences of at least 0.5 J/cm^2 are required (with an ~8-ns IR YAG laser) to minimize the particle size dependence. Above this fluence, there is still a particle size dependence (nonunity range) but it is no longer a function of laser energy. Therefore, this was the approximate fluence used for making soot concentration measurements in the soot generator exhaust.

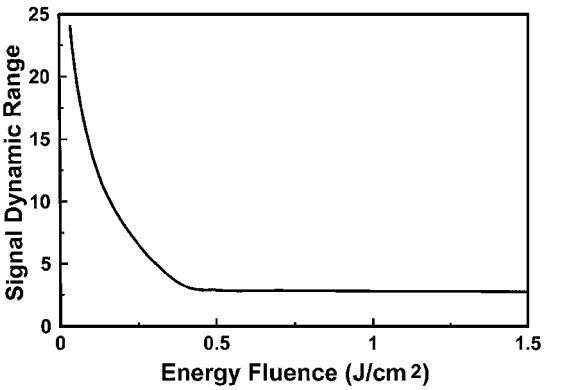

Fig. 3 Model results for the dynamic range of the mass-specific LII signal for a primary particle diameter range of 4–100 nm as a function of illuminating energy fluence (signals detected at 650 nm with 10-nm bandwidth).

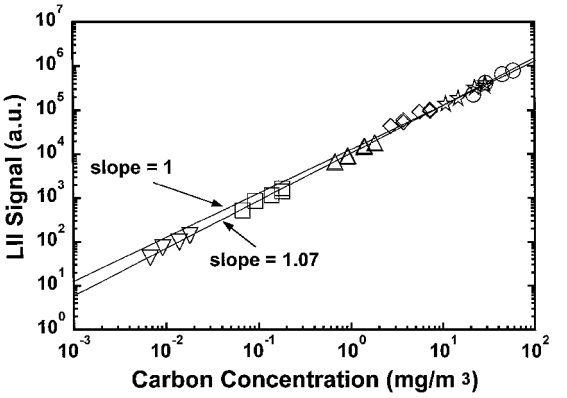

Fig. 4 LII signals measured from the soot generator plotted against calculated carbon concentrations.

Figure 4 shows measured LII signals against soot concentration for concentrations ranging over almost 4 orders of magnitude. The various concentrations were obtained using the four different air dilutions and six different liquid concentrations. The initial carbon solution was diluted, by adding distilled water, to 2, 8, 32, 320, and 3200 times lower concentrations. The temperature at the measurement volume for this case is ~70°C. Concentrations are corrected for the air density (volume flow rate) change due to heating in the dryer. In Fig. 4, each liquid dilution (5.6, 2.7, 0.7, 0.175, 0.0175, and 0.00175 g of C per liter of H_2O) is represented by a unique symbol. The lines represent an ideal dependence of the signal on concentration only and a fit to the data with 315 cm^3/s air dilution. Note the log scaling. The soot concentrations shown in Fig. 4 range from about 8 μg/m^3 to 70 mg/m^3 [~4 parts per trillion (ppt) to 30 parts per billion (ppb)]. At the lowest concentration, the detection system still included a neutral density filter that reduced the signal by one order of magnitude. Therefore, for this system, with a 0.2-cm^3 collection volume, 50-ns gate, and 128-shot averaging, we predict a detection limit close to 1 μg/m^3 (0.5 ppt).

Considering the very large range of carbon concentrations, the LII signal is nearly proportional to soot loading. However, it deviates from a completely linear dependence (slope = 1) and is best fitted by a slope of 1.07, i.e., a signal that scales with concentration to the 1.07 power. Signals are detected over a range of

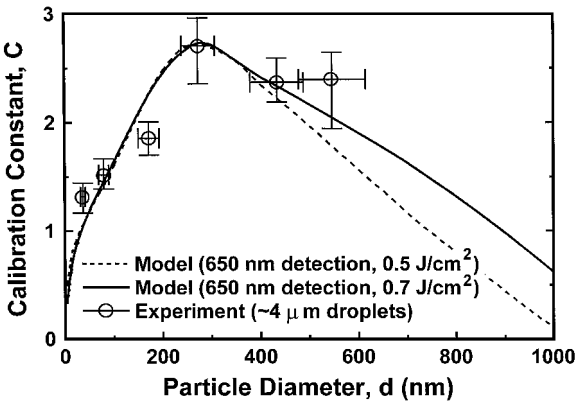

Fig. 5 Particle size dependence of C for Fig. 4 data and from LII model.

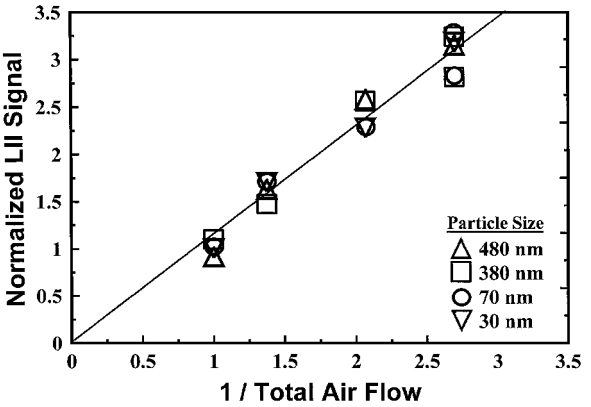

Fig. 6 Signals for the smallest two and largest two particle diameters, corrected by the average calibration constants (from Fig. 5) and normalized by their corresponding solution concentrations (lowest value scaled to 1).

approximately 570–850 nm. The signals are produced by a 250-mJ (~0.5-J/cm^2) pulse at 1064 nm. The best fit line was produced using only measurements with a single air dilution, the maximum. Thus with particle number density held constant, assuming all of the carbon black particles in a droplet coalesce to form one particle as already described, this line represents the behavior of the LII signal as a function of particle size. Using the relation concentration $\propto Nd^3$ to convert this to a size dependence, we would predict for a simple power law dependence (like that of a previous analytic approximation[28]) that the LII signal scales as $d^{3.21}$. However, a more complete numerical model shows that a power law dependence is too simplistic.

To examine the size dependence more closely, we first define the LII calibration constant C by the ratio $C =$ signal/soot concentration. Without a size dependence, C would be a true constant. The effect of particle size is seen in Fig. 5, where C is plotted for both the numerical model (solid line) and experimental results (symbols). Values of C averaged (over air dilutions) and extrema (error bars) are shown for each liquid dilution, and particle size is based on an estimate of the diameter (4 μm) of the liquid droplets produced by the nebulizer. For this comparison, the model signal is calculated for 650-nm detection (10-nm bandwidth) and two energy fluences within the range of the experimental uncertainty. Because the exact spectral response of the PMT was not known, the model result is reported for constant detector responsivity over a small range (645–655 nm), where we expect the combination of detector response and LII emission to peak. Similar calculations near 550 and 750 nm change the result only slightly, shifting the curve horizontally by roughly 50 nm. Because there is some uncertainty in the shape and size of the laser beam, and therefore the effective average energy density, model results are plotted for illuminating intensities at both 0.7 and 0.5 J/cm^2. These model curves are not intended as best fits to the data but simply to compare the overall trends. The experimental values shown are averaged over the various dilution airflow rates for each of the liquid dilutions, with the vertical error bars representing the maximum and minimum of each set.

PDPA measurements of the nebulizer droplet diameter yielded an average value D_{10} of 4 μm, with a 2-μm FWHM for the measured size distribution and 95% of the droplets being less than 10 μm. The best comparison to the modeling results (to the nearest micrometer) is also for a roughly 4-μm water droplet, which yields a soot particle size range of ~35–550 nm. The horizontal error bars represent the particle sizes based on 3.5- and 4.5-μm water droplets. Although the upper part of this soot particle size range is big compared to typical primary particle sizes in engine exhausts (generally <50 nm), it is useful for analyzing the accuracy of the model predictions.

As seen in Fig. 5, both the model and experiments indicate a nonmonotonic size dependence for the LII signal over the large size range studied. The calibration constant increases for small particle sizes and then reaches a peak before falling at larger sizes. The results can be explained as follows: For particles below the Rayleigh limit ($\pi d/\lambda < \sim 1$), absorption heating and radiation emission scales like volume, but the cooling mechanisms scale closer to surface area. Therefore, larger particles reach higher temperatures and emit more signal per unit volume. As particles exceed the Rayleigh limit for emission, the signal per volume ratio will drop. At even larger particle sizes, nonvolumetric absorption will result in lower particle temperatures and, therefore, a further reduced signal per volume ratio. In addition, the quantitative comparison between the model and the experiments is reasonably good, based on the measured water droplet size. Both predict a maximum variation in C of roughly 2.5 times for the particle size range considered here. Returning to the simple power law fit for particle diameters below the peak of the curve (~250 nm), the experimental data scale like $d^{3.45}$ and the model like $d^{3.41}$. For comparison, Melton's approximation[28] suggests a $d^{3.24}$ scaling. However, note that the model may not be predicting the behavior of the smaller particles very well. Alternatively, we may be seeing the result of a limiting effect on the smallest attainable particle sizes.

There is also some variation, ~10%, in C for a given liquid concentration but for the different airflow rates. Because each airflow rate results in a different particle number density and soot residence time in the heater, there is a possibility of agglomeration or similar effect on the LII results that might influence the comparison to the model. For example, low flow rates mean high soot number densities and long residence times and thus more likelihood of agglomeration. Such agglomeration would affect LII from large particles (near or above the Rayleigh limit) more than from small particles. Agglomeration does little to change particle surface area, and therefore particle cooling rates, but could significantly increase the effective optical size of the particle, reducing the heating rate. Such possibilities are examined in Fig. 6, which shows normalized LII signals from the two smallest and two largest particle sizes (or liquid concentrations). The rest of the data yield roughly the same information but, for clarity, are not included.

In Fig. 6, the LII signals for each liquid dilution are corrected for particle size effects using the average C values from Fig. 5. In addition, each point is normalized by its liquid carbon concentration and plotted against the inverse of the total airflow rate for that case. Ideally, this normalization should produce an identical LII signal for all points at a given total airflow rate, and the signal would scale linearly with air dilution. Thus, Fig. 6 represents the variation in the (nominally) size-corrected LII signals as a function only of soot concentration change associated with air dilution. Again, if agglomeration was occurring, we would expect the largest particles to be more likely to fall below the linear fit as the airflow rate decreases (less heating of agglomerated large particles and, therefore, less signal). The variation with air dilution is clearly linear, and the scatter about the best fit line is similar for large and small particles. Although the data do show increased scatter for lower airflow rates, this is most likely a problem associated with repeatability in setting the rotameter at low flow rates. Thus, we conclude that possible residence time and agglomeration effects are negligible under the current operating conditions.

In addition to size dependence, another issue in making quantitative LII measurements is the temperature dependence of the signal. This is important for flows with temperature gradients. Additionally,

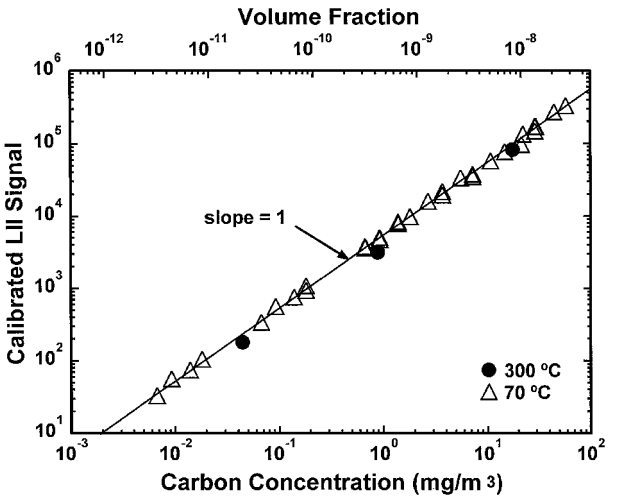

Fig. 7 LII signals, corrected from particle size using the average *C* values from Fig. 5, for the 70°C data of Fig. 4 and for preheated dilution air at three liquid concentrations with a constant air dilution (770 cm^3/s).

it is useful to know whether temperature must be matched when calibrating an LII system for an engine exhaust measurement. Therefore, further measurements were made with the secondary air preheated before it was mixed with the carbon-loaded flow (see Fig. 1). LII signals were acquired at a jet exit temperature of 300°C for three liquid dilutions (1, $\frac{1}{20}$, and $\frac{1}{400}$ strength) and a single air dilution of 770 cm^3/s. Figure 7 shows all the earlier results, at 70°C, along with the higher-temperature data. The plotted carbon concentrations at the jet exit were again corrected for the gas density change at the elevated temperatures. (Recorded temperatures are at the jet exit.) In addition, all of the data were corrected for the size dependence, using a single value of *C* (the average from the 70°C data) for each liquid dilution set. The high-temperature data fall on the same line as the 70°C data. Generally, we would expect the change in gas temperature to lower the conductive cooling rate. Thus, particles would have higher average temperatures and higher signals in the hotter flow. However, because the particles are laser heated to much higher temperatures (>3000 K) than the gas and because of the prompt gating employed, we do not see a significant temperature effect.

Conclusions

In flame experiments, problems have been encountered in attempting to compare the LII signal from soot with the local soot volume fraction because of the influence of other parameters in the combusting environment. Soot concentration levels here were measured using LII in a controllable environment that is also configured to simulate conditions more representative of the exhaust of a typical jet engine. Control over particle size and shape makes the current results more amenable to comparison with the results of standard models. A broadband LII signal has been shown to provide a reasonable measurement of the volume fraction of soot in air over a range of 4 orders of magnitude. The detection limit of the system was estimated to be a soot concentration of ~1 μg/m^3 (~0.5 ppt). This sensitivity is well below the ability of other practical, nonintrusive approaches such as extinction measurements and has many advantages, including real-time response and reduced engine run times, compared with those of intrusive sampling.

Pulsed IR excitation (between 0.5 and 1.0 J/cm^2) and prompt, gated (50-ns) broadband detection were chosen both to produce good sensitivity and to reduce particle size dependence. For a particle size range of ~35–250 nm, the remaining particle dependence results in a variation of about 2.5 times in the LII calibration constant. A similar variation is predicted by a standard LII model, which is based on energy and mass balances for a single spherical primary soot particle, though some deviation is noted for smaller particles. Both model and experiments show a nonmonotonic variation of the calibration constant as particles exceed the Rayleigh limit for emission/absorption. The relative accuracy of the LII model suggests that it can be used to estimate potential systematic errors in flows with variations in soot particle size. Additionally, it may be useful for correcting LII soot concentration measurements if particle sizes can be independently determined.

Except for simple gas density changes, variations of a few hundred Kelvin do not have a significant effect on the LII signal for detection temporally gated near the laser pulse, where the particle temperatures are much higher than the gas temperature and particle cooling is dominated by vaporization. This suggests that temperature variations across an engine exhaust, or between operating conditions, will not affect the LII measurement. Similarly, calibration of an LII system can be performed at a temperature well below that of the exhaust.

In summary, LII shows promise as a relatively simple, sensitive, and accurate method for measuring soot concentrations in engine exhausts over a wide range of conditions. Within the limiting assumption that the LII signal depends only on primary particle size, the standard LII model appears to reasonably predict LII signal variations.

Acknowledgments

This work was supported in part by the National Science Foundation under a CAREER award (CTS-9502371) and by the SBIR program of the Department of Defense. The private communication from C. Beckman, Cabot Corporation, Boston, Massachusetts, Oct. 1998, is gratefully acknowledged.

References

[1]Brouwer, J., Ault, B. A., Bobrow, J. E., and Samuelsen, G. S., "Active Control Application to a Model Gas Turbine Combustor," Gas Turbine and Aeroengine Congress and Exposition, American Society of Mechanical Engineers, Paper 90-GT-326, Brussels, Belgium, June 1990.

[2]Burtscher, H., Schmidt-Ott, A., and Siegmann, H. C., "Monitoring Particulate Emissions from Combustions by Photoemissions," *Aerosol Science and Technology*, Vol. 8, No. 2, 1988, pp. 125–132.

[3]Hartman, P. G., Plee, S. L., and Bennethum, J. F., "Diesel Smoke Measurement and Control Using an In-Cylinder Optical Sensor," *SAE Transactions*, Vol. 100, Sec. 3, 1991, pp. 1259–1272.

[4]Dobbins, R. A., Fletcher, R. A., and Lu, W., "Laser Microprobe Analysis of Soot Precursor Particles and Carbonaceous Soot," *Combustion and Flame*, Vol. 100, No. 1, 1995, pp. 301–309.

[5]Köylü, Ü. Ö., McEnally, C. S., Rosner, D. E., and Pfefferle, L. D., "Simultaneous Measurements of Soot Volume Fraction and Particle Size/Microstructure in Flames Using a Thermophoretic Sampling Technique," *Combustion and Flame*, Vol. 110, No. 4, 1997, pp. 494–507.

[6]Puri, R., Richardson, T. F., Santoro, R. J., and Dobbins, R. A., "Aerosol Dynamic Processes of Soot Aggregates in a Laminar Ethene Diffusion Flame," *Combustion and Flame*, Vol. 92, No. 3, 1993, pp. 320–333.

[7]Santoro, R. J., Yeh, T. T., Horvath, J. J., and Semerjian, H. G., "The Transport and Growth of Soot Particles in Laminar Diffusion Flames," *Combustion Science and Technology*, Vol. 53, No. 2, 1987, pp. 89–115.

[8]Bockhorn, H. (ed.), *Soot Formation in Combustion (Mechanisms and Models)*, Vol. 56, Springer Series in Chemical Physics, Springer–Verlag, New York, 1994.

[9]Adams, K. M., Davis, L. I. J., Jr., Japar, S. M., and Pierson, W. R., "Real-Time *In Situ* Measurements of Atmospheric Optical Absorption in the Visible via Photoacoustic Spectroscopy. II: Validation for Atmospheric Elemental Carbon Aerosol," *Atmospheric Environment*, Vol. 23, No. 3, 1989, pp. 693–700.

[10]Vander Wal, R. L., Zhou, Z., and Choi, M. Y., "Laser-Induced Incandescence Calibration via Gravimetric Sampling," *Combustion and Flame*, Vol. 105, No. 4, 1996, pp. 462–470.

[11]Vander Wal, R. L., and Dietrich, D. L., "Laser-Induced Incandescence Applied to Droplet Combustion," *Applied Optics*, Vol. 34, No. 6, 1995, pp. 1103–1107.

[12]Vander Wal, R. L., and Weiland, K. J., "Laser-Induced Incandescence: Development and Characterization Towards a Measurement of Soot-Volume Fraction," *Applied Physics B*, Vol. 59, No. 4, 1994, pp. 445–452.

[13]Shaddix, C., and Smyth, K., "Laser-Induced Incandescence Measurements of Soot Production in Steady and Flickering Methane, Propane, and Ethylene Diffusion Flames," *Combustion and Flame*, Vol. 107, No. 4, 1996, pp. 418–452.

[14]Quay, B., Lee, T. W., Ni, T., and Santoro, R. J., "Spatially Resolved Measurements of Soot Volume Fraction Using Laser-Induced Incandescence," *Combustion and Flame*, Vol. 97, No. 3–4, 1994, pp. 384–392.

[15]Bengtsson, P.-E., and Alden, M., "Soot Visualization Strategies Using Laser Techniques," *Applied Physics B*, Vol. 60, No. 1, 1995, pp. 51–59.

[16]Ni, T., Pinson, J. A., Gupta, S., and Santoro, R. J., "Two-Dimensional Imaging of Soot Volume Fraction by the Use of Laser-Induced Incandescence," *Applied Optics*, Vol. 34, No. 30, 1995, pp. 7083–7091.

[17]Appel, J., Jungfleisch, B., Marquardt, M., Suntz, R., and Bockhorn, H., "Assessment of Soot Volume Fractions from Laser-Induced Incandescence by Comparison with Extinction Measurements in Laminar, Premixed, Flat Flames," *26th Symposium (International) on Combustion*, Combustion Inst., Pittsburgh, PA, 1996, pp. 2387–2395.

[18]Snelling, D. R., Smallwood, G. J., Campbell, I. G., Medlock, J. E., and Gülder, Ö. L., "Development and Application of Laser-Induced Incandescence (LII) as a Diagnostic for Soot Particulate Measurements," AGARD 90th Symposium of the Propulsion and Energetics Panel on Advanced Non-Intrusive Instrumentation for Propulsion Engines, Brussels, Belgium, Oct. 1997.

[19]McManus, K. R., Frank, J. H., Allen, M. G., and Rawlins, W. T., "Characterization of Laser-Heated Soot Particles Using Optical Pyrometry," AIAA Paper 98-0159, Jan. 1998.

[20]Tait, N. P., and Greenhalgh, D. A., "PLIF Imaging of Fuel Fraction in Practical Devices and LII Imaging of Soot," *Berichte der Bunsengesellschaft für Physikalische Chemie*, Vol. 97, No. 12, 1993, pp. 1619–1625.

[21]Will, S., Schraml, S., and Leipertz, A., "Two-Dimensional Soot Particle Sizing by Time-Resolved Laser-induced Incandescence," *Optics Letters*, Vol. 20, No. 22, 1995, pp. 2342–2344.

[22]Cignoli, F., Benecchi, S., and Zizak, G., "Time-Delayed Detection of Laser-Induced Incandescence for the Two-Dimensional Visualization of Soot in Flames," *Applied Optics*, Vol. 33, No. 24, 1994, pp. 5778–5782.

[23]Dec, J. E., zur Loye, A. O., and Siebers, D. L., "Soot Distribution in a D.I. Diesel Engine Using 2-D Laser-Induced Incandescence," *SAE Transactions*, Vol. 100, Sec. 3, 1991, pp. 277–288.

[24]Case, M. E., and Hofeldt, D. L., "Soot Mass Concentration Measurements in Diesel Engine Exhaust Using Laser-Induced Incandescence," *Aerosol Science and Technology*, Vol. 25, No. 1, 1996, pp. 46–60.

[25]Hess, C. F., "Photothermal Laser Deflection, an Innovative Technique to Measure Particles in Exhausts," Environics Div., Engineering and Services Lab., U.S. Air Force Engineering and Services Center, U.S. Air Force Rept. ESL-TR-90-16, Tyndall AFB, FL, Oct. 1993.

[26]Weeks, R. W., and Duley, W. W., "Aerosol-Particle Sizes from Light Emission During Excitation by TEA CO_2 Laser Pulses," *Journal of Applied Physics*, Vol. 45, 1974, pp. 4661, 4662.

[27]Rohlfing, E. A., "Optical Emission Studies of Atomic, Molecular, and Particulate Carbon Produced from a Laser Vaporization Cluster Source," *Journal of Chemical Physics*, Vol. 89, No. 10, 1988, pp. 6103–6112.

[28]Melton, L. A., "Soot Diagnostics Based on Laser Heating," *Applied Optics*, Vol. 23, No. 13, 1984, pp. 2201–2208.

[29]Hofeldt, D. L., "Real-Time Soot Concentration Measurement Technique for Engine Exhaust Streams," *SAE Transactions*, Vol. 102, Sec. 4, 1993, pp. 45–57.

[30]Eckbreth, A. C., "Effects of Laser-Modulated Particle Incandescence on Raman Scattering Diagnostics," *Journal of Applied Physics*, Vol. 48, No. 11, 1977, pp. 4473–4479.

[31]Dasch, C. J., "Continuous-Wave Probe Laser Investigation of Laser Vaporization of Small Soot Particles in a Flame," *Applied Optics*, Vol. 23, No. 13, 1984, pp. 2209–2215.

[32]Mewes, B., and Seitzman, J. M., "Soot Volume Fraction and Particle Size Measurements with Laser-Induced Incandescence," *Applied Optics*, Vol. 36, No. 3, 1997, pp. 709–717.

[33]Lahaye, J., and Prado, G., "Morphology and Internal Structure of Soot and Carbon Blacks," *Particulate Carbon: Formation During Combustion*, Plenum, New York, 1998, pp. 33–55.

R. P. Lucht
Associate Editor